Tetsuo Isozaki, MD
Kazushi Numata, MD
Takayoshi Kiba, MD
Koji Hara, MD
Manabu Morimoto, MD
Takashi Sakaguchi, MD
Hisahiko Sekihara, MD
Toru Kubota, MD
Hiroshi Shimada, MD
Toshio Morizane, MD
Katsuaki Tanaka, MD

Index terms:
Liver neoplasms, diagnosis, 761.3194, 761.323, 761.332
Liver neoplasms, US, 761.12988
Microbubbles
Ultrasound (US), harmonic study

Published online before print
10.1148/radiol.2293020858
Radiology 2003; *229*:798–805

Abbreviation:
HCC = hepatocellular carcinoma

[1] From the Third Department of Internal Medicine (T.I., T. Kiba, K.H., M.M., T.S., H. Sekihara), Clinical Laboratory (K.N.), and Second Department of Surgery (T. Kubota, H. Shimada), Yokohama City University School of Medicine, Japan; Department of Medicine, Kanagawa Dental College, Yokosuka, Japan (T.M.); and Gastroenterological Center, Yokohama City University Medical Center, Japan (K.T.). Received July 11, 2002; revision requested September 5; final revision received May 2, 2003; accepted May 8. **Address correspondence to** K.N., Gastroenterological Center, Yokohama City University Medical Center, 4–57 Urafune-cho, Minami-ku, Yokohama 232-0024, Japan (e-mail: *kz-numa@zero.ad.jp*).

Author contributions:
Guarantor of integrity of entire study, K.T.; study concepts, T.I., K.T.; study design, K.T.; literature research, K.N., T.I.; clinical studies, T.I., T.S., T. Kubota, M.M.; data acquisition, T.I., K.N.; data analysis/interpretation, K.T., K.H.; statistical analysis, T.M.; manuscript preparation, T.I.; manuscript definition of intellectual content, T. Kiba, T.S.; manuscript editing, H. Sekihara, H. Shimada; manuscript revision/review, K.T., K.N.; manuscript final version approval, K.T.

Differential Diagnosis of Hepatic Tumors by Using Contrast Enhancement Patterns at US[1]

PURPOSE: To assess the accuracy of pattern-based classification of contrast material–enhanced wideband harmonic gray-scale ultrasonographic (US) images in the differential diagnosis of hepatic tumors.

MATERIALS AND METHODS: A total of 183 hepatic lesions in 183 patients were studied; lesions included 116 hepatocellular carcinomas, 42 liver metastases, and 25 liver hemangiomas. After injection of a galactose–palmitic acid contrast agent, lesions were scanned with contrast-enhanced wideband harmonic gray-scale US in the arterial, portal venous, and late venous phases. The enhancement patterns were classified, and multiple logistic regression analysis was used to identify diagnostic patterns that enabled differentiation between hepatic tumors.

RESULTS: Five enhancement patterns were found to be significant in predicting different hepatic tumors. In hepatocellular carcinomas, the presence of intratumoral vessels in the arterial phase and homogeneous or heterogeneous enhancement in the portal phase were the most typical patterns. In metastases, the absence of intratumoral vessels in the arterial phase and ring enhancement or a perfusion defect in the portal phase were the most typical patterns. In hemangiomas, the absence of intratumoral vessels in the arterial phase and peripheral nodular enhancement in the portal phase were the most typical patterns. The sensitivity, specificity, and accuracy of diagnosis based on combinations of enhancement patterns were, respectively, 94.8%, 94.0%, and 94.5% for hepatocellular carcinoma; 90.5%, 94.3%, and 93.4% for metastasis; and 88.0%, 99.4%, and 97.8% for hemangioma.

CONCLUSION: Contrast-enhanced wideband harmonic gray-scale US is a useful tool for differentiating among the hepatic tumors studied.

Color Doppler ultrasonography (US) is a noninvasive method of evaluating the hemodynamic characteristics of hepatic tumors, and analysis of Doppler US spectra within or around tumors is useful for differentiating between malignant and benign tumors (1–5). However, conventional Doppler US often provides limited vascular information because hepatic masses are located deep in the abdomen and are often small or subject to motion artifacts due to respiratory or cardiac activity (6). Contrast agents have been developed to enhance Doppler US signals and overcome these limitations (7); these contrast agents consist of tiny microbubbles that are confined to intravascular spaces and do not leak through the vessel wall. Although they increase the reflectivity of blood and enhance spectral and color Doppler signals, even contrast material–enhanced color Doppler US is associated with artifacts such as color blooming and oversaturation (7,8).

Harmonic US imaging is a new technique that uses microbubble contrast agents and produces fewer artifacts (7,8). Two methods of harmonic US imaging are available: The first method is based on filtering the fundamental component of the received signal (9–12), while the second method is based on a phase cancellation of the fundamental frequency with phase-inverted wideband pulses (13–17). Contrast-enhanced phase-inverted wideband harmonic gray-scale US is a promising new technique that can enable detection of microbubbles with a high level of sensitivity. The advantages of using this wideband

harmonic US imaging technique are the elimination of the fundamental component signal from normal tissue without the need for filtering and the high signal-to-noise ratio of the second harmonic signal obtained after the summation of both received signals, resulting in a high spatial and contrast resolution (18). The excellent sensitivity of this contrast-enhanced wideband harmonic US imaging technique can be used to visualize tumor blood perfusion (13–17), and authors of several earlier studies have assessed the diagnostic performance of contrast-enhanced wideband harmonic US imaging for differentiating among hepatic tumors (13,14).

Numata et al (16) used contrast-enhanced wideband harmonic gray-scale US with SH U 508A to examine hepatocellular carcinoma (HCC) for the presence of intratumoral vessels in the arterial phase and for enhancement patterns in the portal venous phase. They concluded that the presence of intratumoral vessels in the arterial phase and homogeneous or heterogeneous enhancement in the portal phase are helpful in differentiating HCC from other hepatic tumors.

The purpose of our study was to assess the accuracy of using a classification based on patterns of enhancement on wideband harmonic gray-scale US images in the differential diagnosis of hepatic tumors.

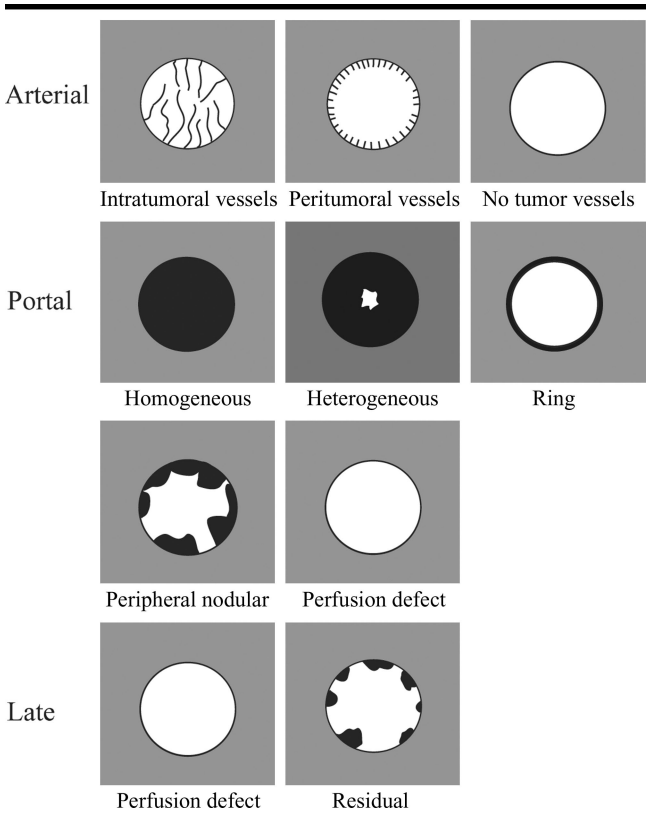

Figure 1. Diagram shows enhancement patterns of hepatic tumors in the arterial, portal, and late phases.

MATERIALS AND METHODS

Patients and Tumors

Between November 1999 and October 2001, we used conventional US to examine 189 consecutive patients with hepatic tumors. All of the patients were admitted to our institutions (Yokohama City University School of Medicine and Yokohama City University Medical Center) and underwent both dual-phase helical computed tomography (CT) and contrast-enhanced wideband harmonic gray-scale US; patients who were suspected of having HCC also underwent angiography. Six patients with six lesions located 10 cm beneath the skin surface were excluded because the increase in attenuation of the ultrasound beam with the increase in depth made it difficult to destroy the microbubbles in such lesions (17). The 183 remaining patients were enrolled in this study. Of these, 138 patients had solitary focal lesions, and 45 patients had multiple focal lesions. When a patient had more than one focal lesion, the largest lesion was evaluated; therefore, 183 hepatic lesions were studied. The patient group consisted of 121 men and 62 women, and there was no significant difference in the mean age (±SD) between men and women (men, 65.3 years ± 9.8; women, 64.0 years ± 9.9).

The final diagnosis of the lesions showed that there were 116 patients with HCC, 42 patients with liver metastasis (10 colon carcinomas, nine pancreatic carcinomas, five gastric carcinomas, four ovarian carcinomas, two malignant melanomas, two nasopharyngeal carcinomas, two esophageal carcinomas, three gallbladder carcinomas, two lung carcinomas, one rectal carcinoma, one laryngeal carcinoma, and one testicular carcinoma), and 25 patients with hemangioma. All HCCs and liver metastases were diagnosed by using histologic examination after surgical resection (four lesions), US-guided biopsy (151 lesions), or autopsy (three lesions). The diagnosis of hemangioma was confirmed by using contrast-enhanced CT and magnetic resonance imaging and by the absence of any changes on follow-up images more than 1 year later. Among those with HCC lesions, 107 of the 116 patients had cirrhosis; this diagnosis was made at histologic and/or clinical examination.

With regard to the age distribution by sex for each tumor type, there were no significant differences in the mean age between men and women among patients with HCC (men, 66.4 years ± 8.3; women, 68.4 years ± 5.4), patients with metastasis (men, 64.5 years ± 11.9; women, 59.3 years ± 8.0), or patients with hemangioma (men, 57.3 years ± 13.1; women, 52.6 years ± 10.6).

The size of each of the hepatic tumors was measured during conventional US by either one of the two operators (T.I., K.N.) who performed the contrast-enhanced harmonic US imaging. The mean maximum diameter was 28 mm ± 18 among HCCs, 34 mm ± 18 among metastases, and 41 mm ± 30 among hemangiomas. All patients gave full informed consent to our study, and approval from our institutional review board was obtained.

We defined early HCC lesions as well-differentiated lesions with no substantial destruction of the preexisting hepatic framework (19).

Procedures

To minimize variations between operators, the contrast-enhanced harmonic US studies were performed by either one of two operators (T.I., K.N.) using the

TABLE 1
Enhancement Patterns of Hepatic Tumors

Enhancement Pattern	HCC	Metastasis	Hemangioma
Arterial phase			
Intratumoral vessels	84 (98/116)*	12 (5/42)*	0 (0/25)*
Peritumoral vessels	12 (14/116)*	60 (25/42)*	24 (6/25)
No tumor vessels	3 (4/116)*	29 (12/42)	76 (19/25)*
Portal phase			
Homogeneous or heterogeneous enhancement	91 (105/116)*	7 (3/42)*	4 (1/25)*
Perfusion defect	8 (9/116)*	43 (18/42)*	0 (0/25)
Ring enhancement	1 (1/116)*	48 (20/42)*	8 (2/25)
Peripheral nodular enhancement	1 (1/116)*	2 (1/42)*	88 (22/25)*
Late phase			
Residual enhancement	33 (38/116)	0 (0/42)*	96 (24/25)*
Perfusion defect	67 (78/116)	100 (42/42)*	4 (1/25)*

Note.—Data are percentages; data in parentheses are numbers of tumors.
* $P < .05$ (χ^2 test).

same examination protocol. Neither operator was aware of the results obtained at helical CT and angiographic examinations or of the diagnosis made at histologic examination. Contrast-enhanced wideband harmonic gray-scale US was performed in all patients. The US examinations were performed with a Sonoline Elegra system (Siemens Medical Systems, Issaquah, Wash) with a 3.5-MHz convex probe. Each liver was imaged with fundamental gray-scale US (transmit, 3.4 MHz; receive, 3.4 MHz) before the patient was administered an intravenous bolus injection of the 300 mg/mL concentration of the galactose–palmitic acid mixture of SH U 508A (Levovist; Schering, Berlin, Germany).

After injection, the liver was scanned by using contrast-enhanced wideband harmonic gray-scale US (transmit, 2.8 or 2.5 MHz; receive, 5.6 or 5.0 MHz) at a frame rate of one to five images per second. The transmission power was 100%, and the mechanical index values were between 1.5 and 1.9. The focus position was set directly below the bottom of the tumor. SH U 508A is a suspension of galactose microparticles (99.9%) stabilized with 0.1% palmic acid. A 7-mL dose of this contrast agent was injected at 0.5 mL/sec via a 20–22-gauge cannula placed in an antecubital vein.

After bolus injection of the contrast agent, 5% glucose was continuously infused at a rate of 5.0 mL/min. The patients gently inspired and then underwent breath-hold imaging for about 30 seconds (20–50 seconds after injection of the contrast agent) while the tumor vessels were examined (observation of the arterial phase). After observing the arterial phase, we froze the recorded images and reviewed them frame by frame from cine loops and stored them on magneto-optical disks. This procedure took approximately 15–35 seconds (mean, 25 seconds), and we used this time to allow pooling of the contrast agent in the hepatic parenchyma. Approximately 80–100 seconds (mean, 90 seconds) after injection of the contrast agent, we observed the tumors for enhancement by using a sweep scan while patients underwent breath-hold imaging for a few seconds (observation of the portal venous phase). After observation of the portal phase, we froze the image again. Finally, 4 minutes after the injection of the contrast agent, we examined the tumor for presence or absence of contrast agent in a sweep scan (observation of the late venous phase). The entire examination was recorded on S-VHS videotape.

Image Evaluation

In the arterial phase, we evaluated the US images for the presence and shape of tumor vessels and classified the patterns of vessels into three categories (Fig 1): intratumoral vessels, peritumoral vessels, or no tumor vessels. In the portal phase, the enhancement patterns of the lesions were classified into four categories (Fig 1): homogeneous or heterogeneous enhancement, perfusion defect, ring enhancement, or peripheral nodular enhancement. In the late phase, the enhancement patterns of the lesion relative to the enhancement pattern in the surrounding liver parenchyma were classified into two categories (Fig 1): perfusion defect or residual enhancement.

The image evaluation was performed independently by two readers (K.T., K.H.). Both readers reviewed all of the US images recorded on S-VHS and magneto-optical disk and were asked to classify each lesion according to the patterns shown in Figure 1. The readers had no knowledge of the results obtained at the helical CT and angiographic examinations or the diagnosis at histologic examination. Nine of the 183 hepatic lesions were classified differently by the two readers; therefore, the two readers and the two operators had a consensus meeting to arrive at the final classification of these nine lesions.

Statistical Analysis

For nominal variables, such as the presence or absence of a certain imaging feature, the rates were compared among the groups by using the χ^2 test. Two-tailed P values of less than .05 were accepted as showing statistical significance.

A multiple logistic regression analysis was performed to select independent variables of imaging features associated with the dependent variable (ie, the tumor type). Since only dichotomous variables can be used as the dependent variable in multiple logistic regression analysis, the dependent variables in our analysis were defined as one of the three tumor types versus the other two (HCC vs metastasis and hemangioma; metastatis vs HCC and hemangioma; hemangioma vs HCC and metastasis). The independent variables were different imaging features observed in the three phases after contrast enhancement: intratumoral vessels, peritumoral vessels, or no tumor vessels in the arterial phase; homogeneous or heterogeneous enhancement, ring enhancement, perfusion defect, or peripheral nodular enhancement in the portal phase; and residual enhancement or perfusion defect in the late phase. Each variable had a dichotomous value (not observed = 0, observed = 1). We selected independent variables with P values of less than .05 in the multiple logistic regression analysis.

Next, we constructed a multivariable model by using these significant independent variables. All tumors exhibited one of the defined combinations of statistically significant independent variables, and these defined combinations were made by using statistically significant independent variables. To evaluate the diagnostic performance of our multivariable model, we calculated the positive predictive values. The positive predictive value of each combined statistically significant independent variables was calculated according to Bayes theorem (20). Where PP is prior probability, *SE* is sensitivity, and *SP* is specificity, positive predictive value was defined as $PP \times SE/[SE \times PP + (1 - SP) \times (1 - PP)]$.

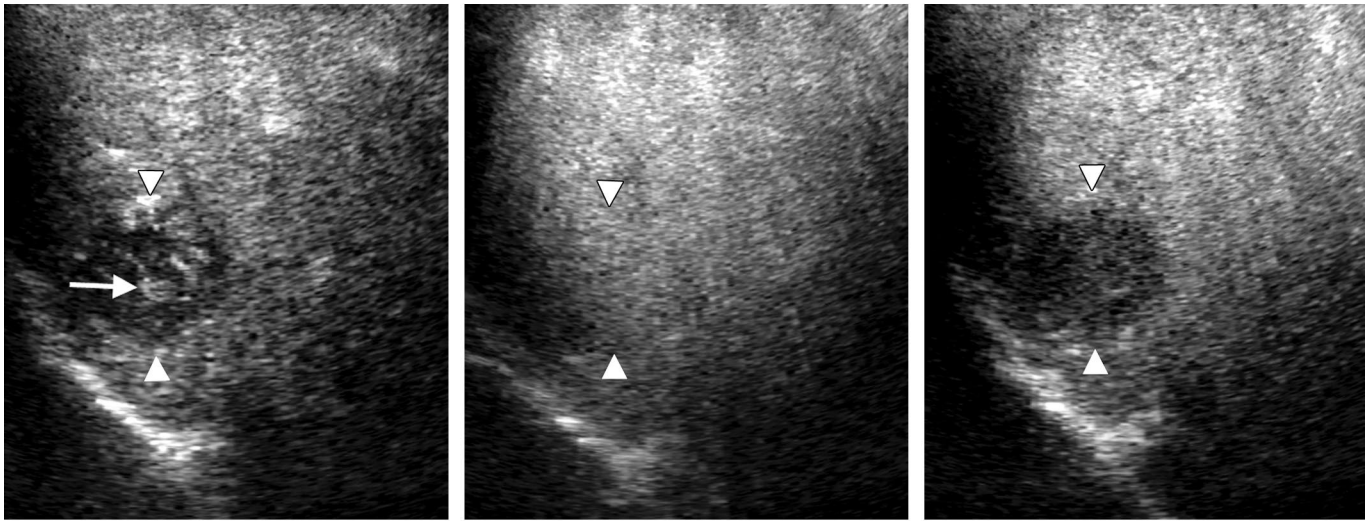

a. b. c.

Figure 2. Intercostal contrast-enhanced wideband harmonic gray-scale US images of the liver in a 52-year-old man with Child class B cirrhosis and HCC (maximum diameter, 30 mm) in the superior anterior segment of the right lobe. Arrowheads point to the margins of the tumor. **(a)** Arterial phase image shows intratumoral vessels that are tortuous centrally (arrow) and peripherally. **(b)** Portal phase image clearly shows homogeneous enhancement of the tumor. Enhancement of normal liver parenchyma is also seen. **(c)** Late phase image shows no contrast enhancement of the tumor. Enhancement of the normal liver parenchyma is seen.

Prior probability was calculated by dividing the numbers of HCCs, metastases, and hemangiomas by the total number of tumors (183 tumors). The diagnosis of each hepatic tumor was made on the basis of the largest positive predictive value of each combined enhancement pattern. Next we summed the number of tumors diagnosed according to their largest positive predictive value and calculated the sensitivity, specificity, and accuracy of each tumor diagnosis based on the results of the enhancement pattern–based classification system already described. We also calculated the sensitivities for differentiating each hepatic tumor by using our multivariable model in the 138 patients with solitary focal lesions (100 patients with HCC, 17 with metastasis, and 21 with hemangioma) and in the 45 patients with multiple focal lesions. The data analysis was performed by using SPSS software (version 10.0J; SPSS, Tokyo, Japan).

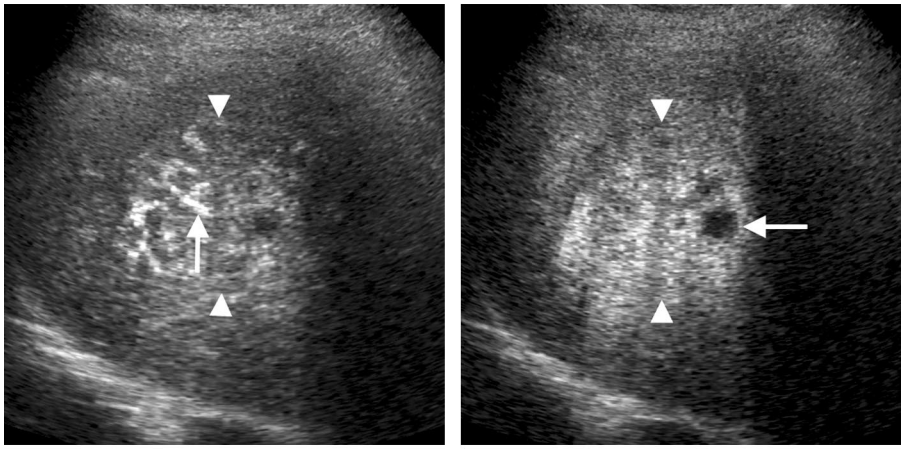

a. b.

Figure 3. Intercostal contrast-enhanced wideband harmonic gray-scale US images of the liver in a 68-year-old woman with Child class A cirrhosis and HCC (maximum diameter, 36 mm) in the superior anterior segment of the right lobe. Arrowheads point to the margins of the tumor. **(a)** Arterial phase image shows intratumoral vessels that are tortuous centrally (arrow) and peripherally. **(b)** Portal phase image clearly shows heterogeneous enhancement of the tumor. Necrotic area (arrow) of the tumor is seen. Enhancement of the normal liver parenchyma is also seen.

RESULTS

Arterial Phase

Table 1 shows the enhancement patterns of hepatic tumors observed by using contrast-enhanced wideband harmonic gray-scale US. In the arterial phase, 98 (84%) of 116 HCC lesions had intratumoral vessels (Figs 2a, 3a). Twenty-five (60%) of 42 liver metastases had fine peritumoral vessels and five (12%) had intratumoral vessels (Fig 4a); no tumor vessels were observed in the remaining 12 metastases (29%). Six (24%) of 25 hemangiomas were enhanced in the peripheral area of the tumor in the arterial phase, and the other 19 (76%) were not enhanced in the arterial phase.

Portal Phase

By using contrast-enhanced wideband harmonic gray-scale US in the portal phase, 105 (91%) of 116 HCC lesions were visualized as isoechoic in comparison with surrounding liver parenchyma (Fig 2b). All of these lesions exhibited a homogeneous or heterogeneous pattern of enhancement: 84 (72%) exhibited a homogeneous pattern (Fig 2b) and 21 (18%) exhibited a heterogeneous pattern (Fig 3b). Since the contrast agent did not enhance the necrotic areas of the tumors,

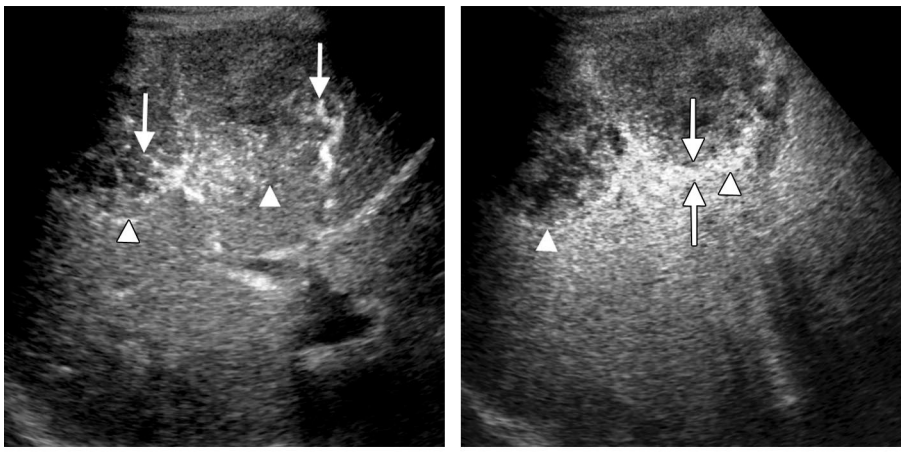

a. b.

Figure 4. Intercostal contrast-enhanced wideband harmonic gray-scale US images of the liver in a 70-year-old man with hepatic metastases (maximum diameter, 60 mm) in the anterior segment of the right lobe, originating from gastric carcinoma. Arrowheads point to the margins of the tumor. **(a)** Arterial phase image shows intratumoral and peritumoral vessels (arrows). **(b)** Portal phase image shows ring enhancement (arrows). Enhancement of the normal liver parenchyma is seen.

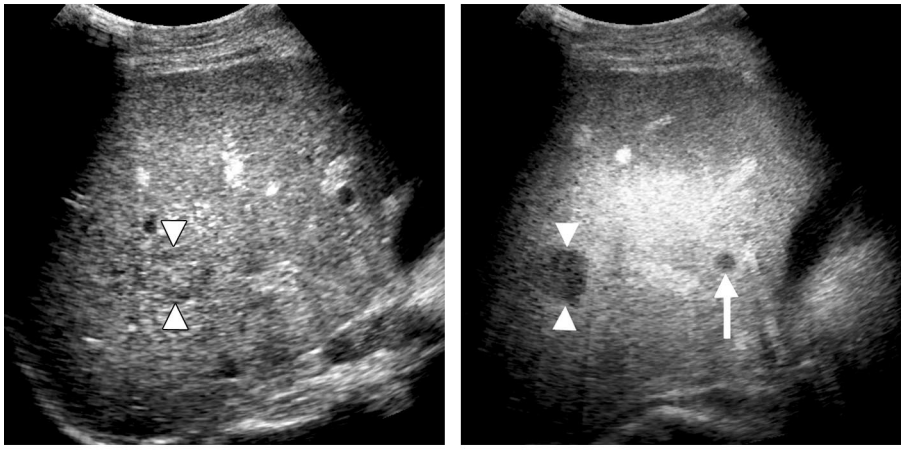

a. b.

Figure 5. Intercostal contrast-enhanced wideband harmonic gray-scale US images of the liver in a 55-year-old man with hepatic metastases (maximum diameter, 22 mm) in the anterior segment of the right lobe, originating from pancreatic carcinoma. Arrowheads point to the margin of the tumor. **(a)** Arterial phase image shows no obvious tumor vessel. **(b)** Portal phase image shows no enhancement of the tumor (perfusion defect). Another hepatic metastasis (arrow) not detected with conventional US is seen. Enhancement of the normal liver parenchyma is seen.

the tumors that included necrotic areas showed a heterogeneous pattern (Fig 3b) (16). Nine (8%) of the 116 HCC lesions showed a perfusion defect in the portal phase. Of these nine lesions that exhibited arterioportal shunting at angiography, four showed a homogeneous pattern of enhancement in the arterial phase but not in the portal phase, and the remaining five lesions were early HCC lesions. One HCC lesion (1%) showed a ring enhancement. The remaining HCC lesion (1%) showed peripheral nodular enhancement. Of 42 liver metastases, 18 (43%) showed a perfusion defect (Fig 5b), 20 (48%) showed ring enhancement (Fig 4b), two (5%) showed homogeneous enhancement, one (2%) showed heterogeneous enhancement, and one (2%) showed peripheral nodular enhancement. Of the 25 hemangiomas, 22 (88%) demonstrated peripheral nodular enhancement (Fig 6b), two (8%) demonstrated ring enhancement, and the remaining lesion (4%) demonstrated homogeneous enhancement.

Late Phase

In the late phase, 78 (67%) of the HCC lesions were visualized as perfusion defects (Fig 2c) and 38 (33%) showed residual enhancement. No residual contrast agent was observed in small HCC lesions (maximum diameter of 20 mm or smaller) in the late phase. All HCC lesions with residual enhancement in the late phase showed intratumoral vessels in the arterial phase. All metastases showed a perfusion defect in the late phase. Of the 25 hemanginomas, 24 (96%) showed residual enhancement in the late phase, and the remaining one (4%) showed a perfusion defect.

Factors Predicting Diagnosis of Hepatic Tumors

On the basis of the results of contrast-enhanced wideband harmonic gray-scale US, multiple logistic regression analysis was performed for nine parameters to determine predictors of the diagnosis of hepatic tumors. Only five parameters were selected as independent variables associated with a type of hepatic tumor (Table 2). Intratumoral vessels (odds ratio, 8.742; $P < .01$) and homogeneous or heterogeneous enhancement (odds ratio, 16.54; $P < .01$) were selected as statistically significant variables to differentiate HCC from the other two types of hepatic lesions combined. Ring enhancement (odds ratio, 103.2; $P < .01$) and perfusion defect (odds ratio, 17.92; $P < .01$) were selected as statistically significant variables to differentiate metastasis from the other two types of lesions combined. Peripheral nodular enhancement (odds ratio, 43.77; $P < .05$) was selected as a statistically significant variable to differentiate hemangioma from the other two types of lesions combined. Two parameters of the late phase were not statistically significant variables.

Enhancement Pattern Classification

Combinations of contrast enhancement patterns in the arterial phase (absence or presence of intratumoral vessels) and portal phase (homogeneous or heterogeneous, ring, peripheral nodular, and perfusion defect) were then analyzed, and eight different combinations of statistically significant predictors in the arterial phase and portal phase were produced (Table 3). Positive predictive value was calculated from the results of

pattern combinations for each hepatic lesion.

The enhancement pattern combinations 1, 5, 7, and 8 showed high positive predictive value for HCC, and pattern 5 was the most predominant among them. The maximum diameter of the HCC lesions in pattern 1 was relatively small (mean, 17 mm ± 3) compared with that of HCC lesions in pattern 5 (mean, 31 mm ± 20), but the difference between them was not significant. All four lesions in pattern 7 were HCCs with arterioportal shunting. The enhancement pattern combinations 2, 3, and 6 showed high positive predictive value for metastasis. Patterns 2 and 3 were the predominant patterns among the three enhancement combinations for the diagnosis of metastasis; however, no significant difference between them was observed with respect to tumor size. Pattern 4 showed high positive predictive value for hemangioma.

The respective sensitivity, specificity, and accuracy of the enhancement pattern–based diagnosis were 94.8%, 94.0%, and 94.5% for HCC; 90.5%, 94.3%, and 93.4% for metastasis; and 88.0%, 99.4%, and 97.8% for hemangioma. When only the solitary focal lesions were analyzed, the sensitivity was 94.0% for HCC, 87.5% for metastasis, and 85.0% for hemangioma. When only the multiple focal lesions were analyzed, the sensitivity was 94.3% for HCC, 94.1% for metastasis, and 100% for hemangioma. No significant differences in sensitivity were observed between solitary lesions and multiple lesions.

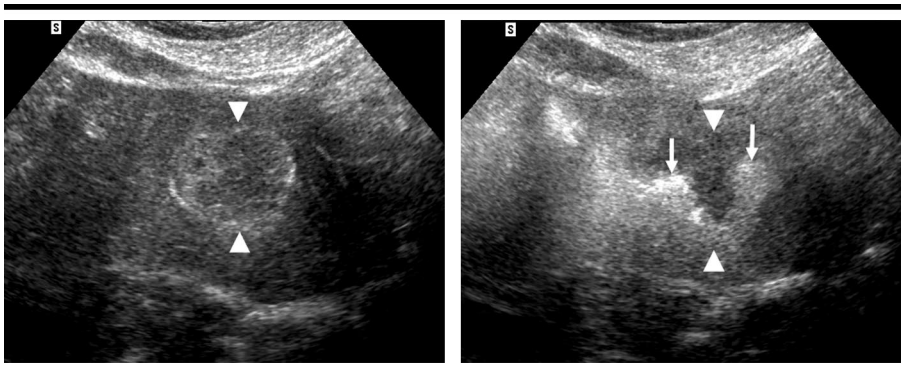

a. **b.**

Figure 6. Transverse contrast-enhanced wideband harmonic gray-scale US images of the liver in a 50-year-old man with hepatic hemangioma (maximum diameter, 39 mm) in the lateral segment of the left lobe. Arrowheads point to the margin of the tumor. **(a)** Arterial phase image shows the absence of any tumor vessel. **(b)** Portal phase image shows peripheral nodular enhancement (arrows). Enhancement of the normal liver parenchyma is seen.

TABLE 2
Logistic Regression Analysis for the Diagnosis of Hepatic Tumors

Parameter	Odds Ratio	95% CI	*P* Value
HCC			
Intratumoral vessels	8.742	1.859, 41.11	<.01
Homogeneous or heterogeneous enhancement	16.54	3.205, 85.39	<.01
Metastasis			
Ring enhancement	103.2	7.311, 14.56	<.01
Perfusion defect	17.92	3.641, 88.20	<.01
Hemangioma			
Peripheral nodular enhancement	43.77	2.342, 818.0	<.05

DISCUSSION

While CT contrast agents disperse into the tissues, US contrast agents do not disperse into the extracellular space, and thus US should permit more accurate demonstration of persistent blood flow in hepatic tumors (21,22). US contrast agents such as SH U 508A can be used even in patients with renal failure and in those who are allergic to iodinated contrast agents. Authors of some earlier studies evaluated contrast-enhanced harmonic gray-scale US with SH U 508A for the differential diagnosis of hepatic tumors (13,14,23). Kim et al (14) evaluated eight HCCs, 33 hepatic metastases, and 20 hepatic hemongiomas by using pulse-inversion harmonic US after injection of SH U 508A, and they found that peripheral globular and rimlike enhancement with progressive centripetal fill-in was useful for the specific diagnosis of hemangioma. Several investigators have reported that, by using pulse-inversion US after injection of SH U 508A, enhancement pattern combined with findings related to the vascular phase, interval-delay vascular phase, and liver parenchyma or postvascular phase are of use in characterizing liver tumors (23,24). Ring enhancement in the vascular phase and a clear defect in the parenchymal or both phases are regarded as positive findings for cholangiocellular carcinoma or metastasis (23). Detectable vascularity, positive enhancement on interval-delay images, and a lack of postvascular enhancement indicate HCC (24).

In our study, the results of multiple logistic regression analysis and the positive predictive values calculated from the results of pattern combinations for each hepatic lesion demonstrated that enhancement pattern–based classification of contrast-enhanced wideband harmonic gray-scale US findings is useful in making the differential diagnosis of hepatic tumors.

In the arterial phase, tumors were classified as having intratumoral, peritumoral, or no tumor vessels (Fig 1), and they were observed mainly in HCCs, metastases, and hemangiomas, respectively. The results in HCCs in which intratumoral vessels were observed in the arterial phase were almost the same as those in our previous study (16). Our results are similar to those of Burns et al (15), who reported marginal or absent tumor vessels but reported no intratumoral vessels in hepatic metastases and hemangiomas with their imaging method.

In our study, in the portal phase more than 90% of HCCs showed homogeneous or heterogeneous enhancement, and more than 90% of metastases showed ring enhancement or perfusion defect. Eighty-five (73%) of the 116 HCCs showed a homogeneous pattern of enhancement in the portal phase; these lesions were visualized as isoechoic and were difficult to identify. Numata et al (25) reported that contrast-enhanced wideband harmonic gray-scale US was useful for diagnosing the viability of HCC after treatment with transcatheter arterial embolization and that it was superior to helical CT for evaluating resid-

TABLE 3
Enhancement Pattern–based Classification for Differentiating Types of Hepatic Tumors

Pattern Combination No.	Enhancement Pattern		Positive Predictive Value			Diagnosis
	Arterial Phase*	Portal Phase	HCC	Metastasis	Hemangioma	
1	Absent	Homogeneous or heterogeneous enhancement	0.929 (12)†	0 (0)	0.0714 (1)	HCC
2	Absent	Ring enhancement	0.048 (1)	0.852 (18)	0.095 (2)	Metastasis
3	Absent	Perfusion defect	0.217 (5)‡	0.783 (18)	0 (0)	Metastasis
4	Absent	Peripheral nodular enhancement	0 (0)	0.044 (1)	0.956 (22)	Hemangioma
5	Present	Homogeneous or heterogeneous enhancement	0.969 (93)	0.0312 (3)	0 (0)	HCC
6	Present	Ring enhancement	0 (0)	1 (2)	0 (0)	Metastasis
7	Present	Perfusion defect	0.969 (4)§	0 (0)	0 (0)	HCC
8	Present	Peripheral nodular enhancement	1 (1)	0 (0)	0 (0)	HCC

Note.—Data in parentheses are numbers of lesions. Diagnosis is made on the basis of the largest positive predictive value for each of the three kinds of tumors in each combination of enhancement patterns.

* Intratumoral vessels are "absent" or "present" in the arterial phase.

† All HCC lesions in pattern 1 showed homogeneous enhancement.

‡ All HCC lesions in pattern 3 were early HCC lesions.

§ All HCC lesions in pattern 7 had arterioportal shunting.

ual HCC because the perfusion images are not limited by iodized oil deposition. Since viable HCC had the same enhancement as liver parenchyma in the portal phase, the investigators could decide where to perform percutaneous ethanol injection after transcatheter arterial embolization. Observation of the portal phase was important to detect viable portions of HCCs after transcatheter arterial embolization or percutaneous ethanol injection therapy.

Of the 116 HCC lesions in our study, four exhibited arterioportal shunting at angiography, and these lesions showed a homogeneous or heterogeneous pattern of enhancement in the arterial phase but not in the portal phase. During the portal phase, these lesions appeared hypovascular compared with the surrounding liver parenchyma, and we believe that the arterioportal shunting caused the contrast agent to be flushed through the area more quickly than usual.

Twenty (48%) of 42 metastases showed ring enhancement in the portal phase and peripheral vessels in the arterial phase. Peripheral ring enhancement in metastases may reflect viable tumor tissue at the periphery of the lesion and fibrosis or necrosis in the center (26,27). The perfusion defect observed in 18 (43%) of 42 metastases may reflect hypovascularity of the lesions.

Yamashita et al (28) reported that the dynamic CT enhancement patterns of cavernous hemangiomas are related to the collective size of their constituent vascular space. They also reported that hemangiomas smaller than 30 mm in diameter were homogeneously enhanced in the arterial-dominant phase (28). In our study, the only hemangioma that showed a homogeneous pattern of enhancement was 20 mm in maximum diameter. However, flow velocity in the capillary tissue of hemangiomas larger than 20 mm in maximum diameter, on the other hand, was very slow (28,29); therefore, it took a long time for the microbubbles to perfuse into every vascular space of the hemangioma.

A multiple logistic regression analysis was used to assess the enhancement pattern classification of hepatic tumors. The enhancement patterns were defined according to the presence of five parameters from the arterial and portal phases that were shown to be statistically significant predictors of tumor diagnosis: The presence of intratumoral vessels and homogeneous or heterogeneous enhancement suggested HCC, ring enhancement and perfusion defect suggested metastasis, and peripheral nodular enhancement suggested hemangioma. The combinations of these statistically significant predictors from the arterial and portal phases enabled a highly accurate differential diagnosis of hepatic tumors. Our results are similar to those in a study performed by Tanaka et al (23), in which US findings for the vascular phase (arterial and portal phases) and the liver parenchymal phase (late phase) were combined without using multivariate logistic regression analysis. In our study, however, the multivariate analysis showed that the parameters in the late phase were not significant predictors of a differential diagnosis. This finding suggests that observation of the vascular phase (arterial and portal phases) is important for obtaining a differential diagnosis of hepatic tumors.

Several investigators have reported that hepatic metastases showed a perfusion defect in the late phase of contrast-enhanced phase-inversion US and that this finding markedly improved the detection of liver metastases identified as isoechoic or subtle lesions with conventional US (30,31). We think that the late phase may be useful for detection of metastases or relatively small HCC lesions because all small HCCs (≤20-mm diameter) exhibited a perfusion defect in the late phase. However, this phase is not of value for differentiating hepatic tumors because the perfusion defect and residual enhancement are not significant predictors for the differential diagnoses of hepatic tumors.

A limitation of this study was that this criterion for diagnosis was not applied prospectively. A prospective study of this enhancement pattern–based classification is needed to confirm its accuracy for the differential diagnosis for hepatic tumors. Furthermore, the proportion of HCC tumors in our study appears to be relatively higher than that in Western countries (32).

In summary, we classified contrast-enhanced wideband harmonic gray-scale US findings in hepatic tumors into combinations of contrast enhancement patterns. The enhancement patterns of hepatic tumors can be accurately identified through the examination of the arterial and portal phase. We conclude that contrast-enhanced wideband harmonic gray-scale US is a useful modality for differen-

tiating among the types of hepatic tumors we studied.

References

1. Taylor KJ, Ramos I, Morse SS, Fortune KL, Hammers L, Taylor CR. Focal liver masses: differential diagnosis with pulsed Doppler US. Radiology 1987; 164:643–647.
2. Tanaka S, Kitamura T, Fujita M, Nakanishi K, Okuda S. Color Doppler flow imaging of liver tumors. AJR Am J Roentgenol 1990; 154:509–514.
3. Numata K, Tanaka K, Mitsui K, Morimoto M, Inoue S, Yonezawa H. Flow characteristics of hepatic tumors at color Doppler sonography: correlation with arteriographic findings. AJR Am J Roentgenol 1993; 160:515–521.
4. Nino-Murcia M, Ralls PW, Jeffrey RB Jr, Johnson M. Color flow Doppler characterization of focal hepatic lesions. AJR Am J Roentgenol 1992; 159:1195–1197.
5. Numata K, Tanaka K, Kiba T, et al. Use of hepatic tumor index on color Doppler sonography for differentiating large hepatic tumors. AJR Am J Roentgenol 1997; 168:991–995.
6. Numata K, Tanaka K, Kiba T, et al. Correlation between hepatic tumor index on color Doppler sonography and tumor vessels on arteriography in large hepatocellular carcinomas. Cancer Detect Prev 1999; 23:496–505.
7. Correas JM, Bridal L, Lesavre A, Mejean A, Claudon M, Helenon O. Ultrasound contrast agents: properties, principles of action, tolerance, and artifacts. Eur Radiol 2001; 11:1316–1328.
8. Harvey CJ, Blomley MJ, Eckersley RJ, Cosgrove DO. Developments in ultrasound contrast media. Eur Radiol 2001; 11:675–689.
9. Kono Y, Moriyasu F, Nada T, et al. Gray scale second harmonic imaging of the liver: a preliminary animal study. Ultrasound Med Biol 1997; 23:719–726.
10. Burns PN. Harmonic imaging with ultrasound contrast agents. Clin Radiol 1996; 51:50–55.
11. Schrope D, Newhouse VL, Uhlendorf V. Simulated capillary blood flow measurement using a nonlinear ultrasonic contrast agent. Ultrason Imaging 1992; 14: 134–158.
12. Ding H, Kudo M, Onda H, Suetomi Y, Minami Y, Maekawa K. Contrast-enhanced subtraction harmonic sonography for evaluating treatment response in patients with hepatocellular carcinoma. AJR Am J Roentgenol 2001; 176:661–666.
13. Wilson SR, Burns PN, Muradali D, Wilson JA, Lai X. Harmonic hepatic US with microbubble agent: initial experience showing improved characterization of hemangioma, hepatocellular carcinoma, and metastasis. Radiology 2000; 215:153–161.
14. Kim TK, Choi BI, Han JK, Hong HS, Park SH, Moon SG. Hepatic tumors: contrast agent-enhancement patterns with pulse-inversion harmonic US. Radiology 2000; 216:411–417.
15. Burns PN, Stephanie RW, Simpson DH. Pulse inversion imaging of liver blood flow: improved method for characterizing focal masses with microbubble contrast. Invest Radiol 2000; 35:58–71.
16. Numata K, Tanaka K, Kiba T, et al. Contrast-enhanced, wide-band harmonic grayscale imaging of hepatocellular carcinoma: correlation with helical computed tomographic findings. J Ultrasound Med 2001; 20:89–98.
17. Ding H, Kudo M, Onda H, et al. Evaluation of posttreatment response of hepatocellular carcinoma with contrast-enhanced coded phase-inversion harmonic US: comparison with dynamic CT. Radiology 2001; 221:721–730.
18. Simpson DH, Chin CT, Burns PN. Pulse inversion Doppler: a new method for detecting nonlinear echoes from microbubble contrast agents. IEEE Trans Ultrason Ferroelectr Freq Control 1999; 46:372–382.
19. Kanai T, Hirohashi S, Upton MP, et al. Pathology of small hepatocellular carcinoma: a proposal for a new gross classification. Cancer 1987; 60:810–819.
20. Degoulet P, Fieschi M. Medical decision support systems. In: Degoulet P, Fieschi M, eds. Introduction to clinical informatics. New York, NY: Springer-Verlag, 1997; 153–168.
21. Solbiati L, Goldberg SN, Ierace T, Dellanoce M, Livraghi T, Gazelle GS. Radiofrequency ablation of hepatic matastases: postprocedural assessment with a US microbubble contrast agent—early experience. Radiology 1999; 211:643–649.
22. Cosgrove DO. Basic principles of the use of microbubbles. In: Dawson P, Cosgrove DO, Grainger RG, eds. Textbook of contrast media. Oxford, England: Isis Medical, 1999; 465–485.
23. Tanaka S, Ioka T, Oshikawa O, Hamada Y, Yoshioka F. Dynamic sonography of hepatic tumors. AJR Am J Roentgenol 2001; 177:799–805.
24. Dill-Macky MJ, Burns PN, Khalili K, Wilson SR. Focal hepatic masses: enhancement patterns with SH U 508A and pulse-inversion US. Radiology 2002; 222:95–102.
25. Numata K, Tanaka K, Kiba T, et al. Using contrast-enhanced sonography to assess the effectiveness of transcatheter arterial embolization for hepatocellular carcinoma. AJR Am J Roentgenol 2001; 176: 1199–1205.
26. Nino-Murcia M, Olcott EW, Jeffrey RB, Lamm RL, Beaulieu CF, Jain KA. Focal liver lesions: pattern-based classification scheme for enhancement at arterial phase CT. Radiology 2000; 215:746–751.
27. van Leeuwen MS, Noordzij J, Feldberg A, Hennipman AH, Doornewaard H. Focal liver lesions: characterization with triphasic spiral CT. Radiology 1996; 201:327–336.
28. Yamashita Y, Ogata I, Urata J, Takahashi M. Cavernous hamangioma of the liver: pathologic correlation with dynamic CT findings. Radiology 1997; 203:121–125.
29. Bollinger A, Butti P, Barras JP, Trachsler H, Siegenthaler W. Red blood cell velocity in nailfold capillaries of man, measured by a television microscopy technique. Microvasc Res 1974; 7:61–72.
30. Blomley MJ, Albrecht T, Cosgrove DO, et al. Improved imaging of liver metastases with stimulated acoustic emission in the late phase of enhancement with the US contrast agent SH U 508A: early experience. Radiology 1999; 210:409–416.
31. Albrecht T, Hoffmann CW, Schmitz SA, et al. Phase-inversion sonography during the liver-specific late phase of contrast enhancement. AJR Am J Roentgenol 2001; 176:1191–1198.
32. Okuda K. Epidemiology of primary liver cancer. In: Tobe T, Kameda H, Okudaira M, et al, eds. Primary liver cancer in Japan. Tokyo: Springer-Verlag, 1992; 3–15.